THE UNIVERSITY OF MICHIGAN

College of Engineering

Department of Mechanical Engineering

Cavitation and Multiphase Flow Laboratory

Report No. 01357-6-T

CAVITATING FLOW PAST TRANSVERSE CYLINDER IN VENTURI DIFFUSER WITH WATER AND MERCURY

3rd Conference on Hydraulics and Hydraulic Machinery

Budapest, Hungary, September 22-27, 1969

by

Frederick G. Hammitt
Dale J. Kemppainen

Financial Support Provided by:

National Science Foundation

Grant No. GK-1889

March 1969

TABLE OF CONTENTS

LIST OF FIGURES

I. INTRODUCTION

In order to obtain relatively rapid cavitation damage in a flow situation approximating that encountered in prototype fluid machinery, experiments have been conducted with a flow geometry wherein a cylindrical pin is placed across the conical diffuser of a cavitating venturi, i.e., the pin axis is normal to the venturi axis (Fig. 1). The pin itself has been used as the damage specimen, although it would also be possible to imbed damage specimens flush with the diffuser wall. The flow geometry approximates that pioneered by Dr. Shal'nev [1] except that in our case the pin is located in a circular rather than a rectangular duct and in the overall positive pressure gradient caused by the diffuser. Some work has been reported by Shal'nev [2] on the effects of both positive and negative pressure gradients in rectangular ducts. We have previously accrued a considerable amount of experience with cavitating flows in conical venturis, including cases where narrow parallel flat-plate damage specimens have been placed in the diffuser portion parallel to the flow [3, e.g.].

Using water as cavitating fluid with a transparent pin and diffuser, high-speed motion pictures have been taken of the flow regime, allowing a calculation of the Strouhal Number for vortex shedding under these conditions. In addition, pressure profiles have been measured around the pin for various cavitation conditions. Some understanding of the location and distribution of damage on the pin can be gained from this study of the flow regime.

With the same flow configuration, damage tests were made in cavitating mercury on stainless steel test specimens. Since we have had considerable previous experinece in this laboratory with cavitation mercury, it was chosen in this particular case in order to obtain more rapid damage. Photographs of the damaged specimens after relatively short exposure show the spatial and size distribution of individual craters as a function of position around the specimen.

II. RESULTS OBTAINED

A. Strouhal Number. It was observed by Hunsaker[4] that the overall cavitation region in a cavitating venturi oscillates in length with the downstream portion periodically detaching and shedding travelling vortices much like a Karman vortex street. This phenomenon could be described in terms of a modified Strouhal Number $S = V/D$, which is a function of the average extent of the cavitating region. Similar observations were reported by Knapp[5] for an ogive in a tunnel test section and by Shal'nev[1] for his rectancular duct with transverse pin geometry. In this latter case, which most closely approximates our present geometry, the Strouhal Number based upon pin diameter and mean velocity at a distance upstream from the pin in his rectangular uniform area duct exhibited an average value ranging from about 0.16 for a non-cavitating flow to a maximum of about 0.24 for extensive cavitation.

A more recent generalized study of vortex-shedding frequencies by Lienhard[6] shows that the Strouhal Number for transverse circular pins in constant area ducts depends somewhat upon Reynolds Number but equals about 0.20 for $10^3 < Re < 10^6$, and increases to about 0.26 as Re increases to 10^7. Hence Shal'nev's results are in the range to be expected according to this later study.

In our own experiments[7] a photographic study of the cavitation field surrounding the cylindrical pin was made using a Fastax high-speed motion picture camera (14,000 frames/second maximum). A transparent plexiglas venturi and cylindrical pin were used (0.510 in. throat diameter, 0.196 in. pin diameter). With this arrangement it was possible to view the cavitation field in a direction along the specimen. Fig. 2 shows the resultant cavitation field around the pin taken in a direction parallel to the pin axis in a sequence of 8 motion picture frames taken at a rate of about 7400 frames/second.

A complete cycle is shown wherein the direction of the cavitating wake shifts from one side of the pin to the other through an arc of about 60^{o}. Fig. 3 shows the cavitation field taken in a direction normal to the pin axis. The mean stream throat velocity was 50 ft./sec., and the cavitation cloud frequency of oscillation 1.935×10^{3} sec.$^{-1}$. Based on pin diameter the Strouhal Number, S = 0.632 at a pin Reynolds Number, $Re_{p} = 5 \times 10^{5}$; based on throat diameter $Re = 1.3 \times 10^{6}$. For either value Lienhard [6] indicates a value from data for constant area test sections of about 0.2,* and as previously mentioned Shal'nev also found values of about this magnitude [1]. Thus the effect of the positive pressure gradient is to considerably increase the frequency of vortex shedding. This may be explicable as a result of increased pressure forces as compared to inertial forces in the region of the cavitating wake due to the pressure increase and velocity decrease induced by the diffuser.

B. Pin Pressure Profiles. A special hollow cylindrical pin with an 0.20 inch diameter wall pressure tap was constructed to measure the static pressure field around the cavitating pin. This was so arranged that it could be rotated as well as moved along its own axis. Thus pressures could be measured both as a function of angle and radial position in the diffuser. Fig. 4 shows a pressure distribution obtained with this decive for various extents of the cavitation cloud, including a condition without cavitation. The throat velocity for this data was 50 ft./sec. and the water temperature $\sim 70\ ^{o}F$. The measured pressure at zero degrees is of course the total stagnation pressure since in this case the pressure tap hole is pointed in the stream direction. On the other hand, the reading at 90^{o} is the static pressure at that point since the tap is there parallel to the stream. The pressures between 90^{o} and 180^{o} are approximately static pressures, since wall velocities in this wake region are of unknown direction but probably small. As indicated

*A recent report by Jones, et. al. [7] confirms this but shows some scattered data showing $S \cong 0.3$ for $Rep = 6 \times 10^{6}$.

in Fig. 4, the minimum pressure is encountered at about the 80° point (approximately a static pressure) regardless of the extent of the cavitation cloud (overall venturi pressure differentials drops which affect the length of cloud at fixed throat velocity are listed on the figure). Thus the minimum pressure is moved somewhat forward of the theoretical expectation for a cylinder in an infinite fluid by the effect of the enclosing geometry. The 80° point is actually that corresponding to the minimum flow area around the pin due to the interaction of the pin geometry with that of the conical diffuser. Comparison with Fig. 2 shows that bubble nucleation probably starts at about 90°. Fig. 4 also shows a substantial pressure recovery behind the pin for the zero-cavitation case, but little recovery for the cavitation clouds of 3/8 and 5/8 in. length. Fig. 2 and 3 correspond to a cloud length of about 0.6 in. While Fig. 4 shows conditions near the venturi centerline, no appreciable difference was found with pressure profiles measured at different venturi radial positions.

C. Damage Type and Distribution. While the front portion of the pin was undamaged in the mercury cavitation tests which were conducted upon AISI Type 304 stainless steel pins, damage appeared to start at about the 80° position, i.e. roughly corresponding to the minimum pressure point, and being somewhat upstream from the apparent initiation of the cavitation cloud (Fig. 2). Damage in this position may be the result of individual random bubbles or perhaps of flow oscillations which may have caused the cavitation initiation point to shift forward for some small portion of a total test. Also a partly damaged specimen may have exhibited a somewhat different pressure and cloud distribution than the observed transparent undamaged specimens. Fig. 5 is a blow-up (X40) of the upstream extent of the damage region in a typical case. It

shows a relatively clean cut-off of damage in the upstream direction.

The distribution of individual pits on a type 304 stainless steel specimen tested in room temperature mercury at 30 ft./sec. throat velocity* is shown in Fig. 6 after 2 minutes exposure. For this short exposure the damage appears to be the result of a random bombardment by individual bubble implosions. As already mentioned damage starts at about 80^{o}, but the maximum pitting density is at about 100^{o} where, according to Fig. 4, pressure recovery is complete. There is less damage in the rear quadrant and almost none near 180^{o} although a few large pits are still observed over most of the rear portion. This may indicate that the flow remains adjacent to the surface up to at least the 100^{o} position so that bubble collapses occur frequently adjacent to the surface in this region. Since the pressure is increasing up to about 100^{o} (Fig. 4) for 3/8 in. cavity to which this corresponds the bubble implosions in this region are more energetic than those further forward. Assuming from the pitting distribution that flow separation may occur at about 120^{o}, bubble collapses near the surface are apparently less frequent in the separated region. Since the pressure is relatively high in this region, they tend to be highly energetic, which is also true since only relatively large bubbles can persist long enough to reach this portion of the pin surrounded by the relatively high pressure wake.

D. Weight Loss Rates. Weight loss versus duration tests were made in room temperature mercury on 304 stainless steel at 25 and 30 ft./sec. throat velocities[7]. It was found that the damage rate gradually decreased over about the first 2 hours of the test and then achieved a relatively constant rate from 2 to 6

* Overall venturi pressure drop = 70 psi, corresponding to 15 psi in. 50 ft./sec. water tests of Fig. 4 according to classical scaling laws. Thus, this mercury test condition should have a 3/8 in. cavity.

hours (Fig. 7 is a typical curve). Actual data are given in ref. 7. However, the constant rates observed from these curves are cross-plotted in Fig. 8 as a function of the overall pressure drop across the venturi. As expected the damage rate is a strong function of venturi pressure drop since this is closely related to the extent of the cavitation cloud (which could not be directly observed in the mercury tests in a stainless steel venturi). The rate versus pressure drop curves have similar shapes for both velocities, exhibiting single maxima at an intermediate pressure drop. It would be expected that the maximum damage rate pressure drops would be proportional to the square of the velocity ratio between tests, and this is seen to be approximately the case, though the damage peak is not precisely defined by the data in either case (55 and 80 psi, respectively, would be consistent with the velocity ratio).

Comparing the maximum damage magnitudes it is seen that the velocity exponent in these tests is 3.7, which is within the range reported by numerous previous investigators using various different geometries. Previous work in which the first author participated using a rotating disc facility[9] showed that the exponent could be expected to be a function of test duration (or extent of previous damage).

III. CONCLUSIONS

A new cavitation test geometry, using a cylindrical pin positioned across the conical diffuser portion of a cavitating venturi, has been described along with preliminary test results. The characteristics of damage rates achieved using room temperature mercury as test fluid and 304 stainless steel as the damage specimen are reported. It is found that the venturi pressure drop required for maximum damage rate scales approximately with the throat velocity squared and that the damage rate increases from the beginning of the test to a relatively constant value during the period of approximately 2-6 hours duration.

Pressure distributions around the pin were measured in water. These were compared with high-speed motion pictures of the cavitation cloud and with the observed damage distribution as a function of radial position on the pin. Maximum damage was seen to occur near the apparent initiation point of the cloud though some damage was observed upstream of this position. Less damage was observed in the separated region of the downstream quadrant of the pin, although numerous large individual pits were also seen there.

For mercury on stainless steel the initial form of the damage was observed to be that of locally randomly distributed individual pits, presumably each the result of a single bubble implosion.

The high-speed motion pictures showed the cavitation cloud to oscillate from side to side with a Strouhal frequency of 0.632 as compared with a value of about 0.2 observed by Shal'nev in a constant area rectangular duct geometry. The substantially higher Strouhal Number is presumably the result of the strong positive pressure gradient induced by the venturi diffuser.

ACKNOWLEDGEMENTS

Financial support for this work was provided under NSF Grant No. GK-1889, and fellowship support for Mr, Kemppainen by AEC.

BIBLIOGRAPHY

1. K. K. Shal'nev, "Experimental Study of the Intensity of Erosion due to Cavitation", Proc. Symp. on Cavitation in Hydrodynamics, N. P. L. (Teddington), H. M. S. P. Publication, 22 p. 1 to 22 p. 37, 1955.

2. K. K. Shal'nev, "The Influence of a Pressure Gradient in a Flow on the Development of Cavitation Zones", (trans. from) Zhurnal Prikladnoy Mekhaniki i Tekhnicheskoy Fiziki, No. 1, pp. 106-108, 1961.

3. F. G. Hammitt, "Damage to Solids Caused by Cavitation", Phil. Trans. Roy. Soc. A, n. 1110, v. 260, 245-255, 1966.

4. J. C. Hunsaker, "Progress Report on Cavitation Research at MIT", Trans. ASME, 37, 423-424, 1935.

5. R. T. Knapp, "Recent Investigations of the Mechanics of Cavitation Damage", Trans. ASME, 77, 1045-1054, 1955.

6. J. H. Lienhard "Synopsis of Lift, Drag, and Vortex Frequency Data for Rigid Circular Cylinders", Bulletin No. 300, Washington State Univeristy, College of Engr. Research Division, 1966.

7. D. J. Kemppainen, "Prestress Conditioning and its Effects on Material Attrition in a Cavitating Environment", Professional Engineering Degree Dissertation, Nuclear Engr. Department, University of Michigan, 1969 (in preparation), also available as ORA Report 01357-5-T, University of Michigan, 1969.

8. G. W. Jones, J. J. Cincotta, R. W. Walker, "Aerodynamic Forces on a Stationary and Oscillating Circular Cylinder at High Reynolds Numbers", NASA TR R-300, Feb., 1969.

9. G. M. Wood, L. K. Knudsen, and F. G. Hammitt, "Cavitation Damage Studies with Rotating Disk", Trans. ASME, J. Basic Engr., 89, D, 1, 98-110, 1967.

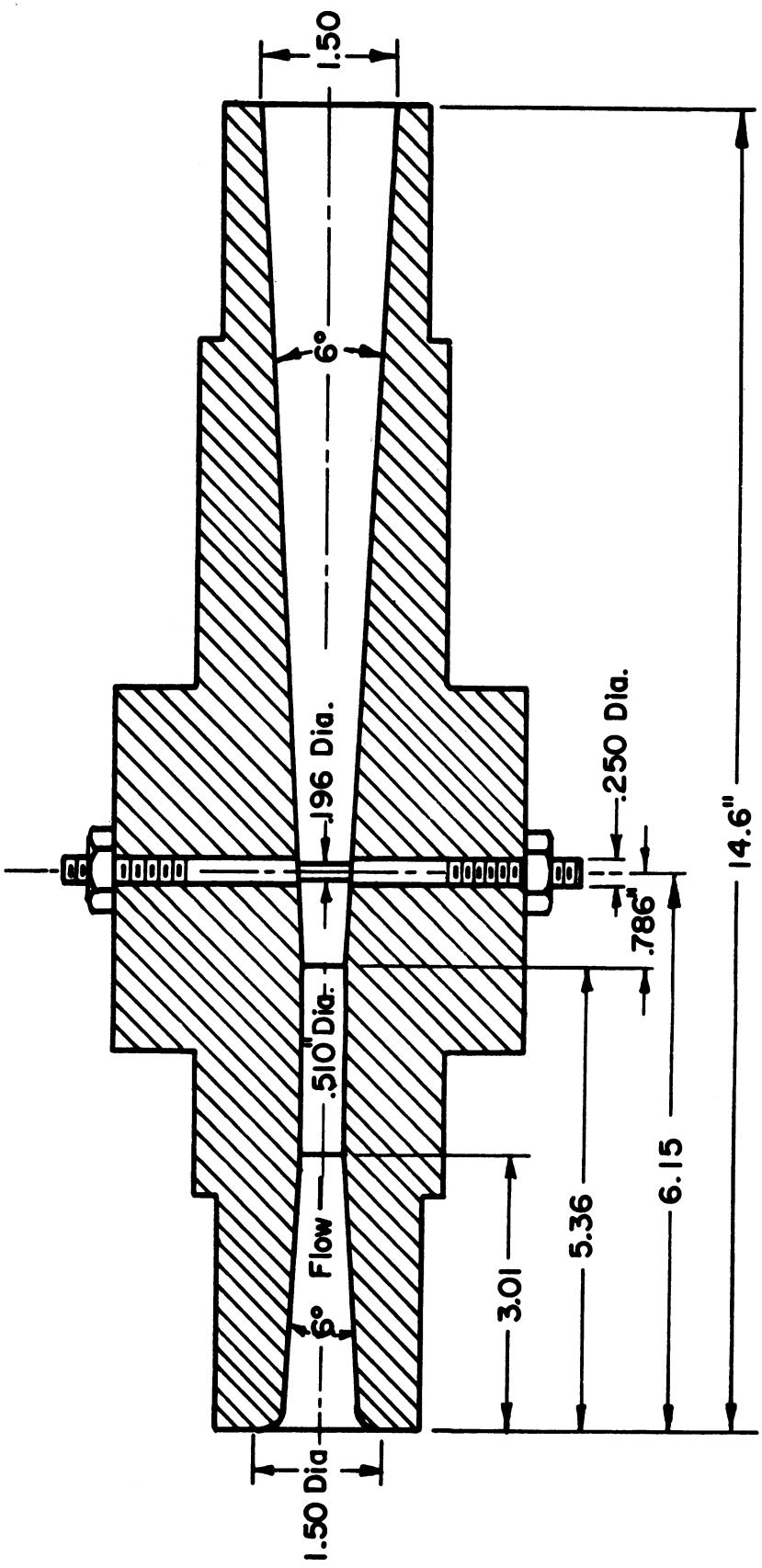

Fig. 1. Dimensioned Venturi Flow Path.

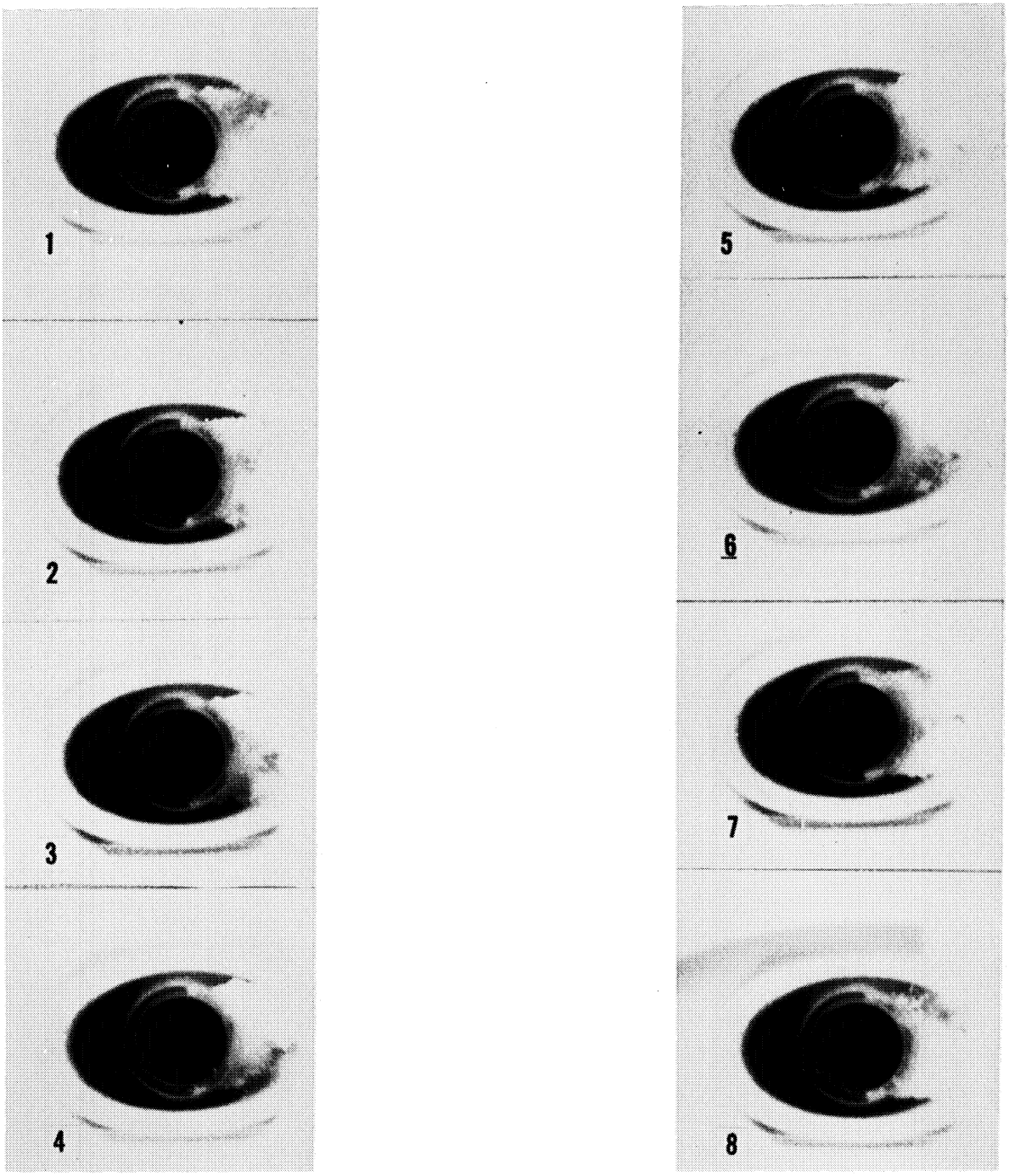

Fig. 2. Motion Picture Frames of Cavitation Field Behind Pin.

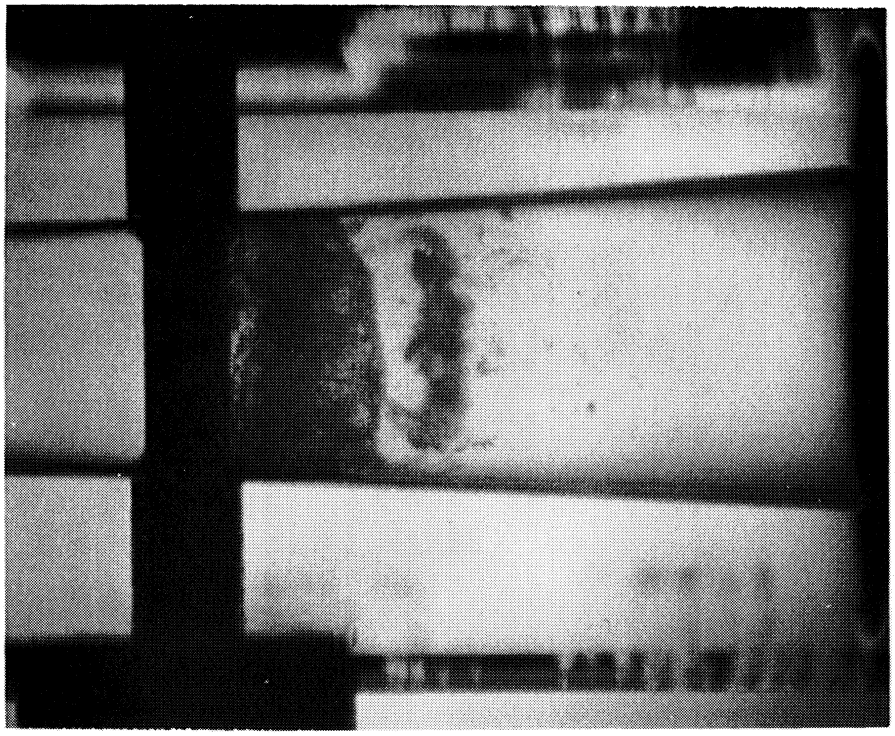

2590

Fig. 3. Photo of Cavitation Field Normal to Pin Axis.

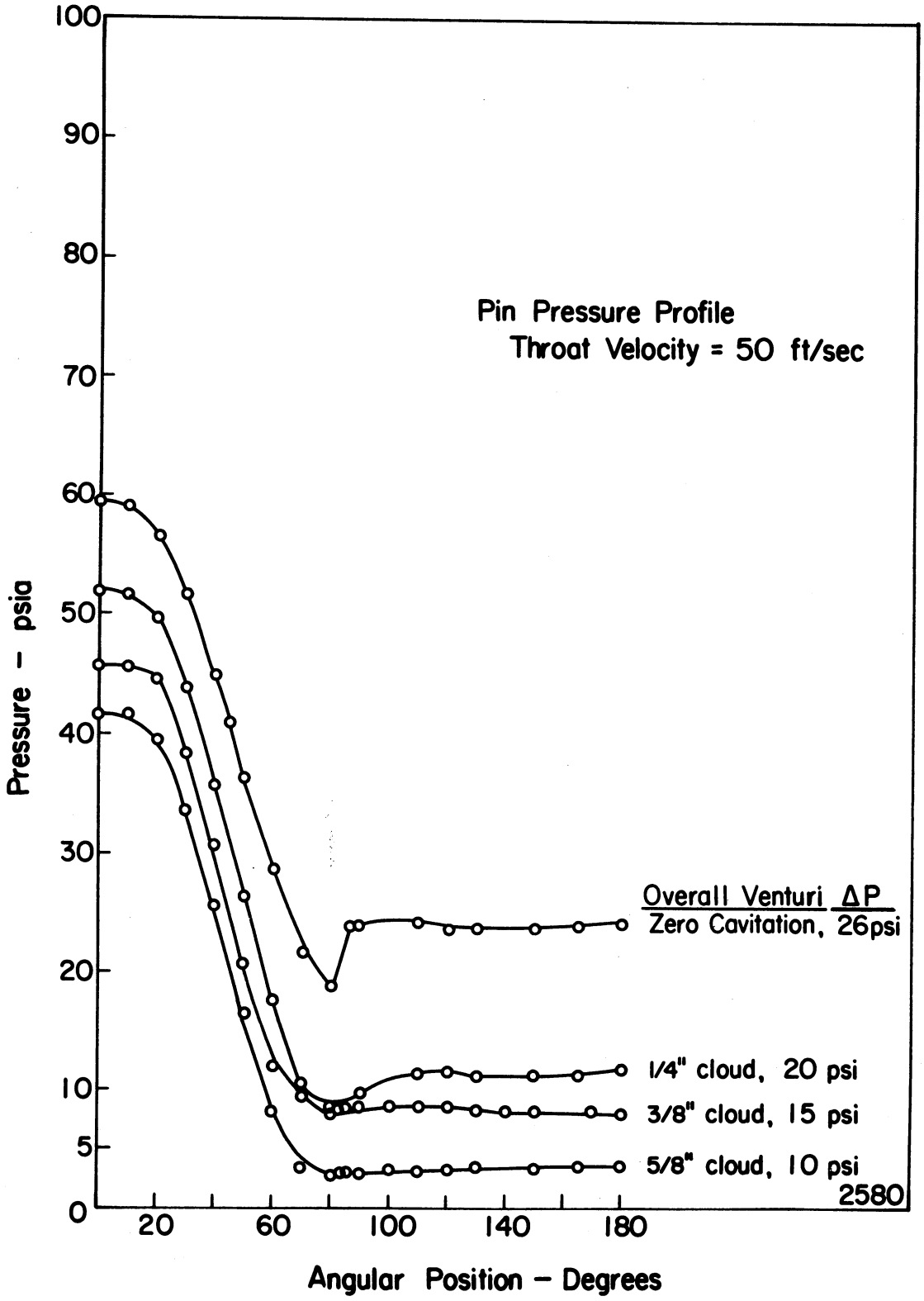

Fig. 4. Pin Pressure Profiles.

Fig. 5. Magnified View of Front Portion of Damage on Pin.

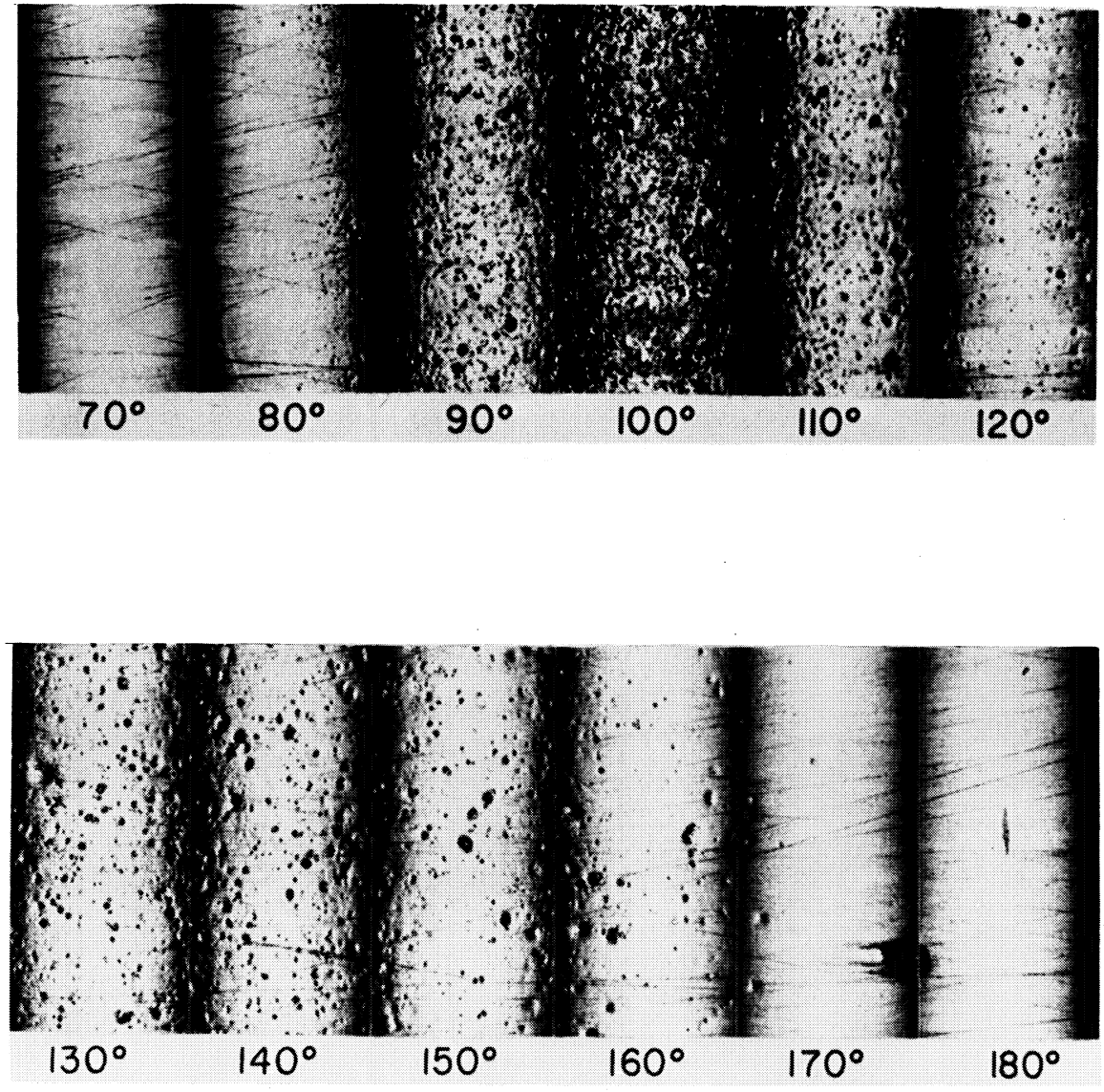

Fig. 6. Damage Distribution on Pin.

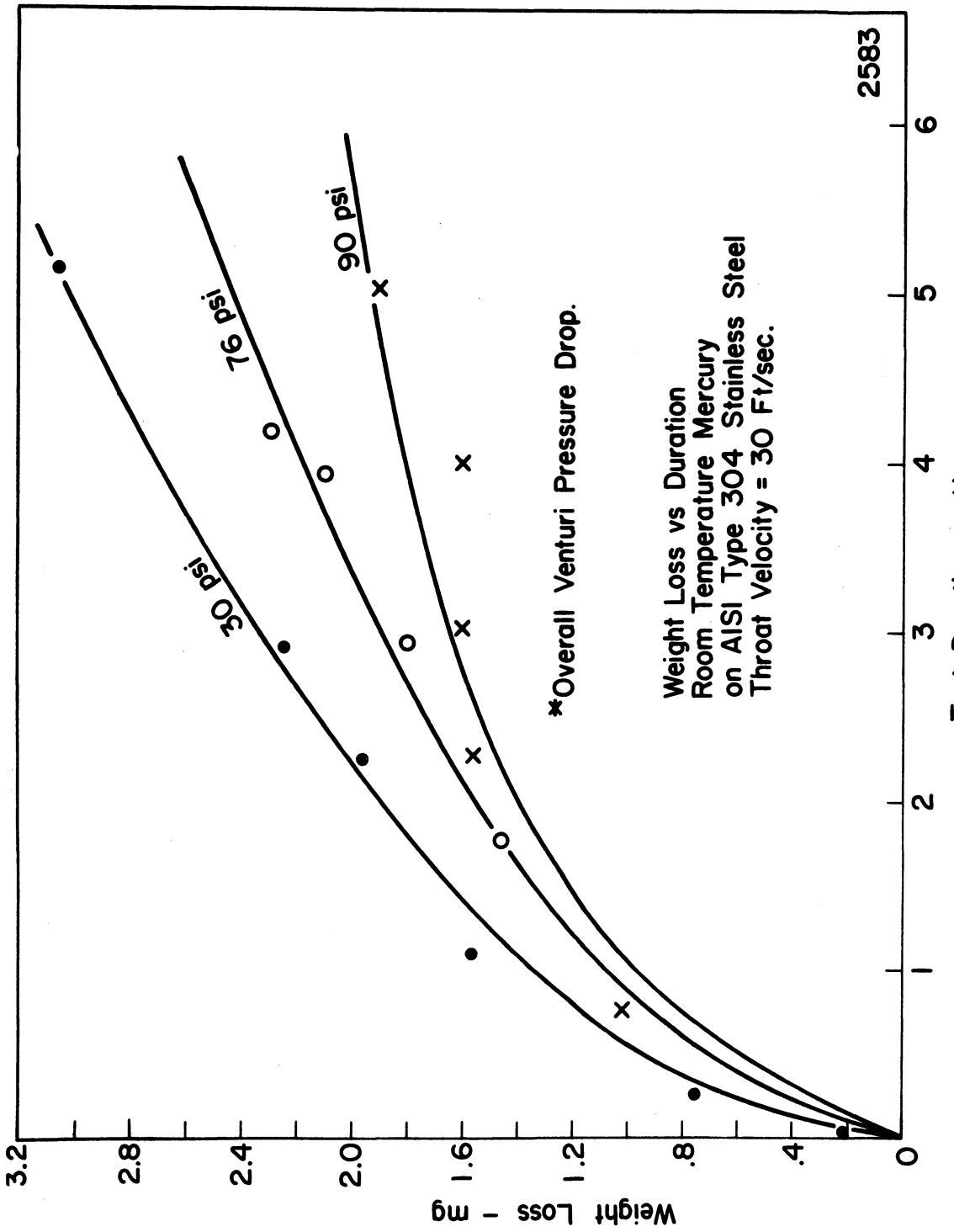

Fig. 7. Typical Time versus Weight Loss Curve.

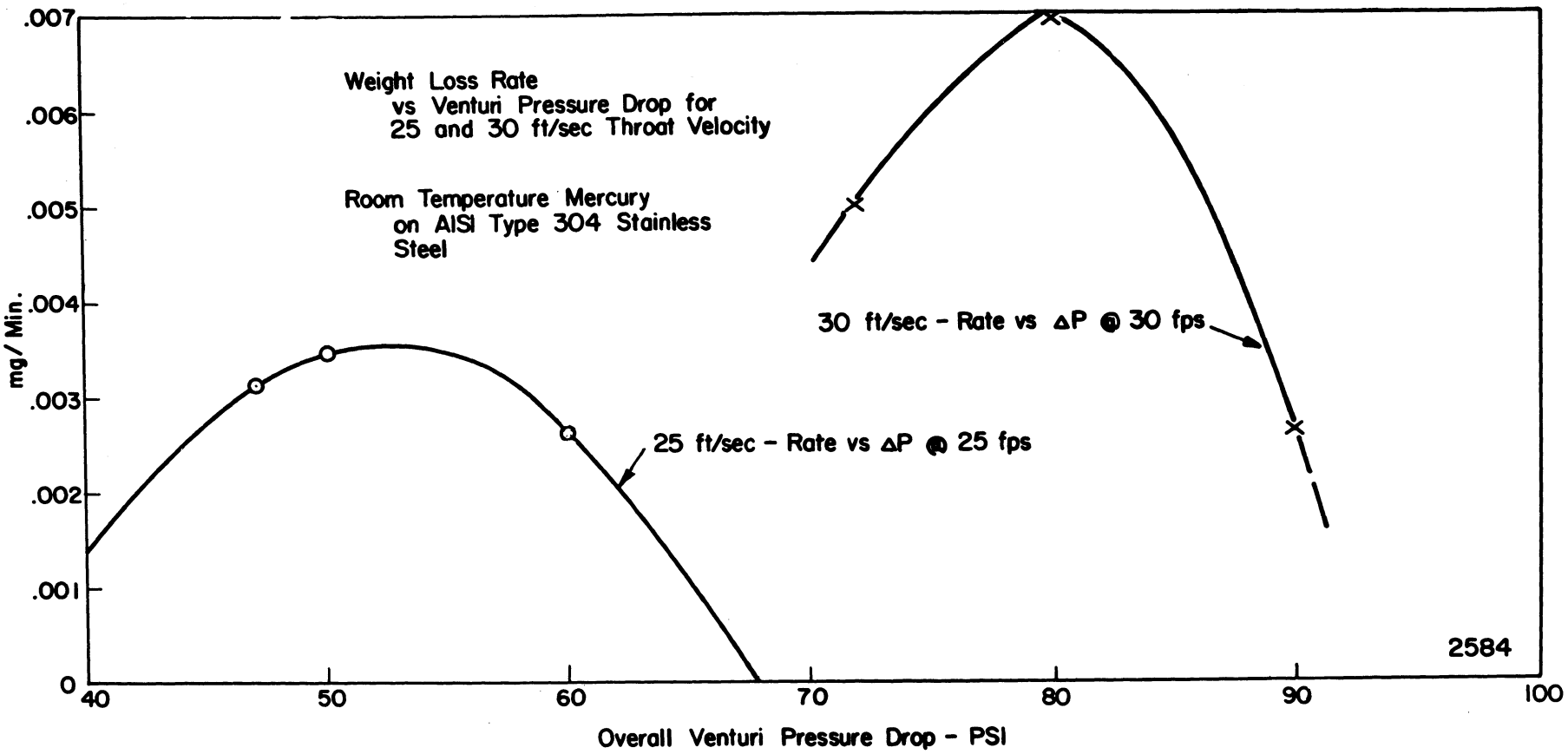

Fig. 8. Weight Loss versus Venturi Pressure Drop.